Title

NON-UNIFORMITIES IN THE MOTION OF A DISLOCATION THROUGH A RANDOM DISTRIBUTION OF POINT OBSTACLES

Authors

Guyot, P.
Stefansky, T.
Dora, J.E.

Publication Date

1967-09-01

UCRL-17848
e.2

University of California

Ernest O. Lawrence Radiation Laboratory

NON-UNIFORMITIES IN THE MOTION OF A DISLOCATION THROUGH A RANDOM DISTRIBUTION OF POINT OBSTACLES

P. Guyot, T. Stefansky, and J. E. Dorn

September 1967

DISCLAIMER

Submitted to Phil. Mag.

UCRL-17848
Preprint

UNIVERSITY OF CALIFORNIA

Lawrence Radiation Laboratory
Berkeley, California

AEC Contract No. W-7405-eng-48

NON-UNIFORMITIES IN THE MOTION OF A DISLOCATION THROUGH A RANDOM DISTRIBUTION OF POINT OBSTACLES

P. Guyot, T. Stefansky and J. E. Dorn

September, 1967

NON-UNIFORMITIES IN THE MOTION OF A DISLOCATION THROUGH A RANDOM DISTRIBUTION OF POINT OBSTACLES

P. Guyot, T. Stefansky and J. E. Dorn

Inorganic Materials Research Division, Lawrence Radiation Laboratory, and Department of Mineral Technology, College of Engineering, University of California, Berkeley, California

September, 1967

ABSTRACT

A theoretical approach to the statistics of cutting randomly distributed point obstacles is presented. The motion of a dislocation can be analyzed in terms of non-uniformities in the breaking away from obstacles over the whole range of obstacle strengths. The elastic limit at 0°K is deduced as a function of the obstacle strength.

I. INTRODUCTION

Most models for dislocation motion past localized obstacles have been erected by assuming that the obstacles can be represented by an ordered arrangement on the slip plane. In contrast, however, many types of obstacles are actually more or less randomly distributed over the slip plane. A statistical treatment of the motion of a dislocation through a random distribution of penetrable obstacles has been recently presented by Kocks (1966)(1967). His analysis revealed that the theoretically deduced flow strength of metals for cutting randomly dispersed obstacles is significantly different from that expected from a regular distribution. The elastic limit at 0°K as calculated by Kocks is in fair agreement with the computer experiments of Foreman and Makin (1966).

The latter authors noted that dislocation motion is not uniform but often takes place by an "unzipping" mechanism involving successive breakaway from obstacles on the dislocation. Non-uniform dislocation motion has been observed experimentally by Suzuki (1967). We will present in this paper a statistical model of the unzipping process and from it deduce the elastic limit at 0°K. Some of the basic elements of the statistical theory have already been introduced by Kocks (1966) (1967) and several new features, not previously considered, emerge from the present treatment.

II. STATISTICS OF THE MODEL

The following assumptions are made in an attempt to emphasize statistical features without encumbering the model with ancillary details:

1. Only one type of simple obstacle of width D is considered and these are assumed to be distributed at random on the slip plane. Let ℓ_s^2 be the average area of the slip plane per obstacle, where $\ell_s^2 \gg D^2$.

2. The force to cut an obstacle at 0°K is taken as $F = \alpha\Gamma$ where α is the strength factor of the obstacle and Γ the average line tension. This force can also be expressed in terms of the breaking angle, ψ_c, between the arms of the dislocation arrested at the obstacle as $F = 2\Gamma \cos \psi_c/2$.

3. Elastic anisotropy, the elastic interaction between the arms of the dislocation line and differences in line tension between edge and screw components of the dislocation are neglected.

4. Under an applied stress, τ, a dislocation moves in its slip plane until it is arrested at neighboring pairs of obstacles. Each arrested dislocation segment is assumed to bow out to a uniform radius of curvature

$$R = \frac{\Gamma}{\tau b}$$

regardless of the proximity of other dislocations (Fig. 1).

The obstacle B is a near neighbor of the randomly chosen obstacle A, when there are no obstacles in the cross-hatched area of Fig. 1.

In terms of probability this leads to a distribution function:

$$P(\phi)\, d\phi \propto e^{-\frac{R^2}{\ell_s^2}(\phi - \sin\phi\cos\phi)} \frac{2R \sin\phi\, d(2R \sin\phi)}{\ell_s^2} \qquad (1)$$

where the first term expresses the condition that there are no obstacles in the bowed-out area, and the second term is proportional to the

probability of finding obstacle B between $r = 2R \sin \phi$ and $r + dr$ from obstacle A.

The statistics of the motion of a dislcoation through a two dimensional random distribution of point obstacles are now introduced: a dislocation will cut a contacted obstacle if the force on the latter, due to the line tension of the dislocation, exceeds $\alpha\Gamma$. A possible cutting configuration is shown in Fig. 2a. The probability of occurrence of this cutting configuration is simply to have no obstacle in the cross-hatched area and therefore is proportional to:

$$C(\phi_1) = e^{-\frac{R^2}{\ell_s^2}(\phi_1 - \sin \phi_1 \cos \phi_2)} \times e^{-\frac{R^2}{\ell_s^2}(\phi_2 - \sin \phi_2 \cos \phi_2)} \qquad (2)$$

with

$$\phi_2 = \pi - (\phi_1 + \psi_c)$$

The average cutting probability, P_c, i.e. the fraction of obstacles transparent to a dislocation at any given stress, is deduced by averaging $C(\phi_1)$ linearly over all permissible values of ϕ_1 as outlined in Appendix 1 (values of ϕ_1 (or ϕ_2) less than $\pi/2 - \psi_c$ lead to cutting configurations represented on Fig. 2b). Therefore P_c is equal to:

i.

$$P_c = \frac{e^{-\frac{R^2}{\ell_s^2}(\pi-\psi_c)} \int_0^{\pi-\psi_c} \frac{R^2}{2\ell_s^2} [\sin 2\phi_1 - \sin 2(\phi_1 + \psi_c)] \, d\phi_1}{\pi - \psi_c}, \qquad (2a)$$

for $\psi_c > \pi/2$;

and ii.

$$P_c = \frac{\left\{ 2 \int_0^{\frac{\pi}{2} - \psi_c} e^{-\frac{R^2}{\ell_s^2}(\phi_1 - \frac{1}{2}\sin 2\phi_1)} e^{-\frac{R^2}{\ell_s^2}[\frac{3\pi}{2} - 2\pi_c - 2\phi_1]} d\phi_1 + e^{-\frac{R^2}{\ell_s^2}(\pi - \psi_c)} \int_{\frac{\pi}{2} - \psi_c}^{\frac{\pi}{2}} e^{\frac{R^2}{2\ell_s^2}[\sin 2\phi_1 - \sin 2(\psi_c + \phi_1)]} d\phi_1 \right\}}{\pi - \psi_c} \quad (2b)$$

for $\psi_c < \pi/2$.

P_c as defined by Eqs. (2a) and (2b) is shown in Fig. 3 as a function of $\ell_s/R = \tau b \ell_s/\Gamma$ over the whole range of obstacle strengths. The variation of P_c with the strength of the obstacle is a physical requirement and constitutes one of the principal points of departure from the formulation presented by Kocks (1967).

A dislocation is arrested at an obstacle when the force due to its line tension is less than $\alpha\Gamma$. Parameters defining these stable configurations can be evaluated using the distribution function given by Eq. (1). As an example, the geometrical average link length, defined as the mean separation between neighbors averaged over all stable configurations (from Eq. (1) and Fig. 4), will be estimated by

$$\bar{r} = \overline{\sqrt{r_1 r_2}} = \frac{\int\int_{\text{stable configurations}} 2R\sqrt{\sin\phi_1 \sin\phi_2}\, \underline{P}(\phi_1)\, P(\phi_2)\, d\phi_1 d\phi_2}{\int\int_{\text{stable configurations}} P(\phi_1)\, P(\phi_2)\, d\phi_1 d\phi_2} \quad (3)$$

From the integration limits given in Appendix 1, it follows that:

when $\psi_c > \pi/2$

$$\bar{r} = \frac{\int_0^{(\pi - \psi_c)} \int_0^{(\pi - \psi_c - \phi_2)} 2R \sqrt{\sin \phi_1 \sin \phi_2}\, e^{-\frac{R^2}{\ell_s^2}(\phi_1 + \phi_2 - \frac{1}{2}\sin 2\phi_1 - \frac{1}{2}\sin 2\phi_2)} \cdot \sin 2\phi_1 \sin 2\phi_2 \, d\phi_1 d\phi_2}{\int_0^{(\pi - \psi_c)} \int_0^{(\pi - \psi_c - \phi_2)} e^{-\frac{R^2}{\ell_s^2}(\phi_1 + \phi_2 - \frac{1}{2}\sin 2\phi_1 - \frac{1}{2}\sin 2\phi_2)} \sin 2\phi_1 \sin 2\phi_2 \, d\phi_1 d\phi_2} \tag{4a}$$

when $\psi_c < \pi/2$

$$\bar{r} = \frac{\left\{ \int_0^{\frac{\pi}{2} - \psi_c} \int_0^{\frac{\pi}{2}} 2R \sqrt{\sin \phi_1 \sin \phi_2}\, e^{-\frac{R^2}{\ell_s^2}(\phi_1 + \phi_2 - \frac{1}{2}\sin 2\phi_1 - \frac{1}{2}\sin 2\phi_2)} \cdot \sin 2\phi_1 \sin 2\phi_1 \, d\phi_1 d\phi_2 + \int_{\frac{\pi}{2} - \psi_c}^{\frac{\pi}{2}} \int_0^{(\pi - \psi_c - \psi_2)} 2R \sqrt{\sin \phi_1 \sin \phi_2}\, e^{-\frac{R^2}{\ell_s^2}(\phi_1 + \phi_2 - \frac{1}{2}\sin 2\phi_2 - \frac{1}{2}\sin 2\phi_2)} \sin 2\phi_1 \sin 2\phi_2 \, d\phi_1 d\phi_2 \right\}}{\left\{ \int_0^{(\frac{\pi}{2} - \psi_c)} \int_0^{\frac{\pi}{2}} e^{-\frac{R^2}{\ell_s^2}(\phi_1 + \phi_2 - \frac{1}{2}\sin 2\phi_1 - \frac{1}{2}\sin 2\phi_2)} \sin 2\phi_1 \cdot \sin 2\phi_2 \, d\phi_1 d\phi_2 + \int_{\frac{\pi}{2} - \psi_c}^{\frac{\pi}{2}} \int_0^{(\pi - \psi_c - \phi_2)} e^{-\frac{R^2}{\ell_s^2}(\phi_1 + \phi_2 - \frac{1}{2}\sin 2\phi_1 - \frac{1}{2}\sin 2\phi_2)} \sin 2\phi_1 \sin 2\phi_2 \, d\phi_1 d\phi_2 \right\}} \tag{4b}$$

Calculated reduced link lengths as a function of $\frac{\ell_s}{R} = \frac{\tau b \ell_s}{\Gamma}$ are shown in Fig. 5 for several obstacle strengths. As with P_c, the variation of $\bar{r}/\ell_s$ with α is physically reasonable and is another departure from the formulation presented by Kocks (1967).

III. THE UNZIPPING MECHANISM

The unzipping mechanism is approximated by the model given in Fig. 6 where a dislocation is shown arrested along a line of obstacles. Under an applied stress τ each dislocation segment bows out with the uniform radius of curvature $R = \frac{\Gamma}{\tau b}$. We assume that the cutting condition $2\Gamma \cos \frac{\psi_c}{2} = \alpha\Gamma$ is satisfied at some obstacle S and that other obstacles are distributed symmetrically about S. To approximate this situation we suggest that they be spaced symmetrically at A, B, C,...,A', B', C',... and separated by the average link length. Once the dislocation cuts through the source obstacle S, it will automatically proceed further if the cutting conditions at A, B, C...,A', B', C'...,are consecutively satisfied, i.e., the dislocation can move by "unzipping".

In the formulation of the unzipping mechanism two distinct cases arise:

1. Single Source (or Non-Interferring Sources)

The dislocation has started to release at the source S and we consider, for the time being, its motion to the right of S. The upper boundary of the area A_1^* is an arc with radius of curvature $R = \frac{\Gamma}{\tau b}$ such that the cutting condition $2\Gamma \cos \frac{\psi_c}{2} = \alpha\Gamma$ is satisfied at obstacle "A". Thus "A" will be cut by unzipping if there are no obstacles in the area A_1. The probability of this event is

$$P_{u1} = e^{-A_1/\ell_s^2} \tag{5a}$$

Similarly, the area A_2^* is such that the cutting condition is satisfied at obstacle "B". The probability that there are no obstacles in A_2 is

$$P_{u2} = e^{-A_2/\ell_s} \tag{5b}$$

Therefore, the probability that "B" is cut by unzipping is $P_{u1}\ P_{u2}$. Since the same area A_2 is associated with the remaining obstacles the probabilities of succeeding events follow directly. Once the dislocation cuts the source obstacle, the total number of obstacles cut by unzipping is:

$$i = \{1 + 2P_{u1} + 2P_{u1}P_{u2} + 2P_{u1}P_{u2}^2 + \ldots\}$$

$$i = \left(1 + \frac{2P_{u1}}{1-P_{u2}}\right) \tag{6}$$

The factor of 2 appears since, once the source acts, the unzipping can proceed in both directions with equal probability.

2. Interferring Sources

When sources are a finite distance apart the unzipping of each can overlap and the number of cut obstacles per source is no longer given by Eq. (6). The fraction (P_c/ℓ_s) of the obstacles are sources and therefore the distance between sources along a line is (ℓ_s/P_c). The unzipping mechanism is now based on the model shown in Fig. 7. The probability that A will be cut by unzipping is P_{u1}

*The areas A_1 and A_2 are evaluated in Appendix 2.

when the unzipping originates at S and $P_{u1}P_{u2}^{(1/P_c - 2)}$* when it originates at S'. Therefore the probability that A is cut by unzipping from the source S only, is $P_{u1}[1 - P_{u1}P_{u2}^{(1/P_c - 2)}]$. Similarly, the probability that B is cut by unzipping from S only is $P_{u1}P_{u2}[1 - P_{u1}P_{u2}^{(1/P_c - 3)}]$. The total number of obstacles cut by unzipping, per source, now is

$$i = 1 + 2 \sum_K P_{u1}P_{u2}^{K-2} (1 - P_{u1}P_{u2}^{1/P_c - K})$$

$$\text{with } K = 2, 3, \ldots, 1/P_c. \qquad (7)$$

Fractional values of $1/P_c$ are treated by averaging over integral values as outlined in Appendix 3. For large values of $1/P_c$, corresponding to sources far apart, Eq. (7) reduces to Eq. (6) which applies for non-interferring sources.

In order to calculate the total area swept out by a dislocation per source, in addition to unzipping along the line joining the sources, the forward motion of the dislocation has to be considered. As a first approximation we assume that the number of new obstacles met by each unzipped dislocation segment resulting from its forward motion is proportional to the ratio of the unzipped arc length divided by the average arc length. Referring to Fig. 7, the average arc length is $2R\phi$,

$$\text{where } \phi = \sin^{-1} (\bar{r}/2R).$$

---

*Unzipping originating at S' reaches A by cutting A' with probability P_{u1} and each of the remaining $(1/P_c - 2)$ obstacles B', C', ..., C, B with probability P_{u2}.

The unzipped arc length associated with a source S is $R(\pi - \psi_c) = 2R\phi_c$, with a neighboring obstacle of type A, $R(\phi_c + \phi)$, and with an obstacle of type B, $2R\phi$. Therefore, from Eq. (7), the total number of obstacles contacted, per source S, becomes

$$j = \frac{\phi_c}{\phi} + 2P_{u1}(1-P_{u1}P_{u2}^{1/P_c-2})\left(\frac{\phi_c+\phi}{2\phi}\right) + 2\sum_{K=3}^{K=1/P_c} P_{u1}P_{u2}(1-P_{u1}P_{u2}^{1/P_c-K}) \quad (8)$$

In Fig. 8, i and j are plotted as functions of $\frac{\ell_s}{R}$ for several obstacle strengths. This is another new feature not considered by Kocks that emerges from this approach: i and j are not constants but vary with α and the stress. The total area swept out by a dislocation per successful cutting can now be written as

$$A = \ell_s^2 \{i + (jP_c)i + (jP_c)^2 i + \ldots = \ell_s^2 \left(\frac{i}{i-jP_c}\right) \quad (11)$$

the term $i\ell_s^2$ is the area swept out by unzipping along the line connecting the sources. The term jP_c is the number of new sources among the j new obstacles contacted and $(jP_c)i\ell_s^2$ is the area swept out by unzipping that originates at the jP_c new sources. The meaning of the remaining terms follows directly.

As previously shown by Kocks (1966), yielding occurs when a dislocation sweeps across the entire slip plane. In terms of this model, the flow stress at 0°K is then given by $jP_c = 1$, and is readily determined from Eqs. (2) and (8). Our values for the flow stress $(\ell_s/R) = \tau b\ell_s/\Gamma$ at 0°K are shown in Fig. 9 together with the results of Kocks (1967) and of Foreman and Makin (1966), over the whole range of obstacle strength.

IV. CONCLUSIONS

A new formulation of the statistical theory for the glide of a dislocation through a random array of point obstacles has been presented. The macroscopic flow stress at 0°K is deduced on the basis of non-uniformities in the motion of the dislocation, namely an unzipping process. The overall agreement with the computer experiments of Foreman and Makin reinforce the following features:

1. The dependence of the statistical parameters such as the cutting probability, as well as the link length or the number of obstacles cut or contacted, on both stress and strength of the obstacles is physically reasonable.

2. The dislocations are expected to remain essentially straight for weak obstacles and to zig-zag between strong obstacles. Our formulation of the unzipping mechanism, based essentially on a straight line model, yields satisfactory results, over the whole range of obstacle strengths. It seems therefore that the motion of a zig-zagged dislocation statistically approximates the motion of a quasi-straight dislocation (i.e. with obstacles placed on a line), implying that zig and zag configurations are equally probable.

3. A bowing-out process (introduced through P_c, when $\psi_c < \pi/2$ (Fig. 2b) begins to contribute for strong obstacles ($\psi_c < \pi/2$), as previously observed by Kocks (1967).

4. The small but increasing disagreement with Foreman and Makin at high obstacle strengths might be attributed to the formation of loops around groups of closely spaced obstacles.

ACKNOWLEDGMENTS

This research was conducted as part of the activities of the Inorganic Materials Research Division of the Lawrence Radiation Laboratory of the University of California, Berkeley, and was done under the auspices of the U. S. Atomic Energy Commission.

APPENDIX 1

The limiting values of ϕ_1 and ϕ_2 are readily obtained from Fig. A.1. Equation $\phi_1 = \pi - \psi_c - \phi_2$ represents the critical cutting condition. The shaded areas in Fig. A.1 correspond to the bowing-out process (Fig. 2b) and are forbidden ranges for stable configurations.

APPENDIX 2

The areas A_1 and A_2 are obtained from Fig. A.2.

For $\psi_c < \pi/2$

$$A_1 = R^2 \left[\pi - \frac{3}{2}\psi_c - 2\phi + \frac{1}{2}\sin\psi_c - 2(1 - \cos\frac{\psi_c}{2})^2 \cot\frac{\psi_c}{2}\right] \quad (A.2.1)$$

$$A_2 = R^2 \left[\sin 2\phi + 2\sin\phi\cos(\phi + \psi_c)\right] \quad (A.2.2)$$

where $\phi = \sin^{-1}\bar{r}/2R$

For $\psi_c > \pi/2$

$$A_1 = R^2\left[\frac{\pi}{2} - \frac{\psi_c}{2} - \phi\right] + \frac{R^2}{2}\left[\sin\psi_c + \sin 2(\psi_c + \phi)\right] - 4R^2 \frac{[\sin(\psi_c + \phi) - \cos\frac{\psi_c}{2}]^2 \cos\frac{\psi_c}{2}\sin(\psi_c + \phi)}{2\cos(\frac{3\psi_c}{2} + \phi)} \quad (A.2.3)$$

A_2 is still given by Eq. (A.2.2).

APPENDIX 3

(a) For $1/P_c = 1$, all sources lie adjacent to each other as shown in Fig. A.3.1 and therefore Eq. (7) reduces to $i = 1$.

(b) For $1/P_c = 2$, all sources again lie adjacent to each other with the configuration shown in Fig. A.3.2. Equation (7) once more reduces to $i = 1 + 2P_{ul}(1 - P_{ul}) = 1$, because $P_{ul} = 1$. In order to distinguish between cases (a) and (b) we will consider all configurations characterized by $1 \leq 1/P_c \leq 3$ as the arithmetic mean of configurations with $1/P_c = 1$ and $1/P_c = 3$. Thus,

$$\{j\}_{1 < 1/P_c < 3} = f\{j\}_{1/P_c = 1} + (1 - f)\{j\}_{1/P_c = 3}$$

with $f.1 + (1 - f)\,3 = 1/P_c$.

In practice, this averaging procedure is used for $1 < 1/P_c < 3$. In all other cases, graphical interpolation yielded satisfactory results.

REFERENCES

Foreman, A. J. E. and Makin, M. J. (1966): Phil. Mag. 14, 911.

Kocks, U. F. (1966): Phil. Mag. 13, 541.

Kocks, U. F. (1967): Can. J. Phys. 45, 737.

Suzuki, T. (1967): Dislocation Dynamics, McGraw-Hill, New York, to be published.

FIGURE CAPTIONS

Figure 1. A neighboring pair of obstacles.

Figure 2. Possible cutting configurations (a) $\psi_c > \pi/2$; (b) $\psi_c < \pi/2$. For ϕ_1 less than $\pi/2 - \psi_c$.

Figure 3. Probability for cutting.

Figure 4. A stable configuration.

Figure 5. Reduced average link length.

Figure 6. Unzipping model.

Figure 7. Unzipping model with interferring sources.

Figure 8. The number of obstacles cut (i) and contacted (j) per unzipping process.

Figure 9. Flow stress at 0°K.

Figure A.1. Limiting values of ϕ_1 and ϕ_2.

Figure A.2. Areas A_1 and A_2.

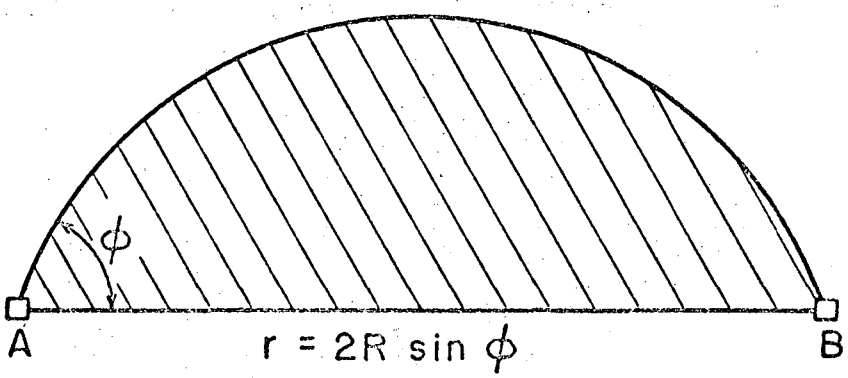

Fig. 1

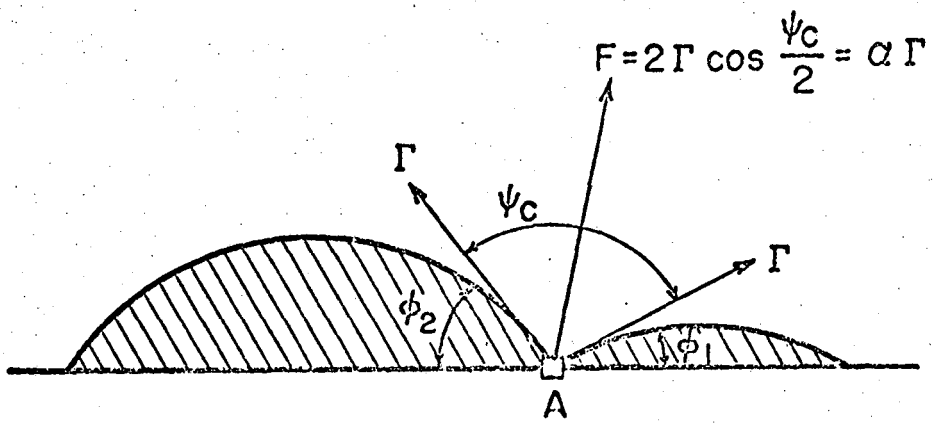

a.

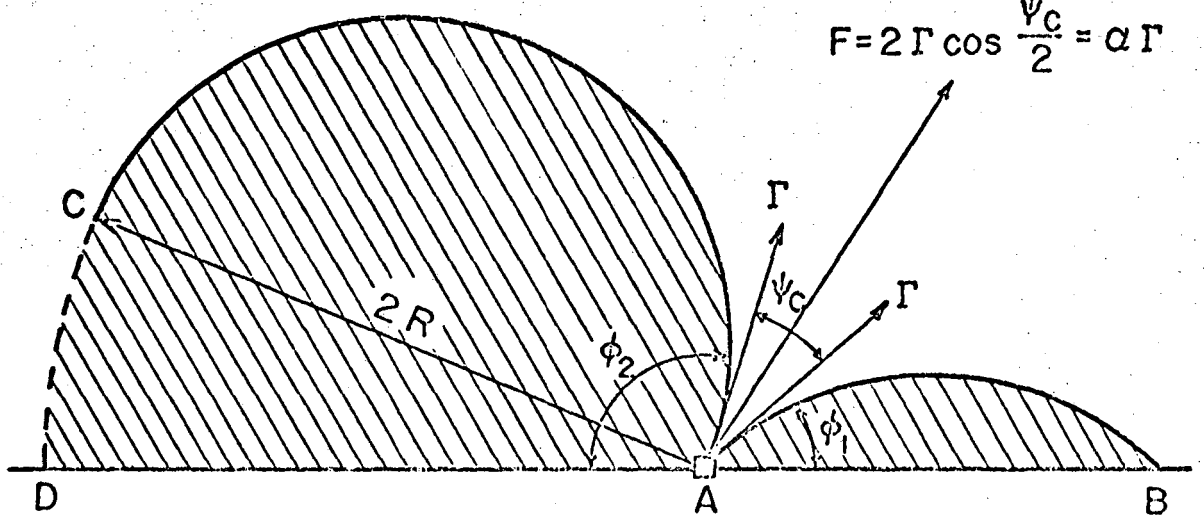

b.

Fig. 2

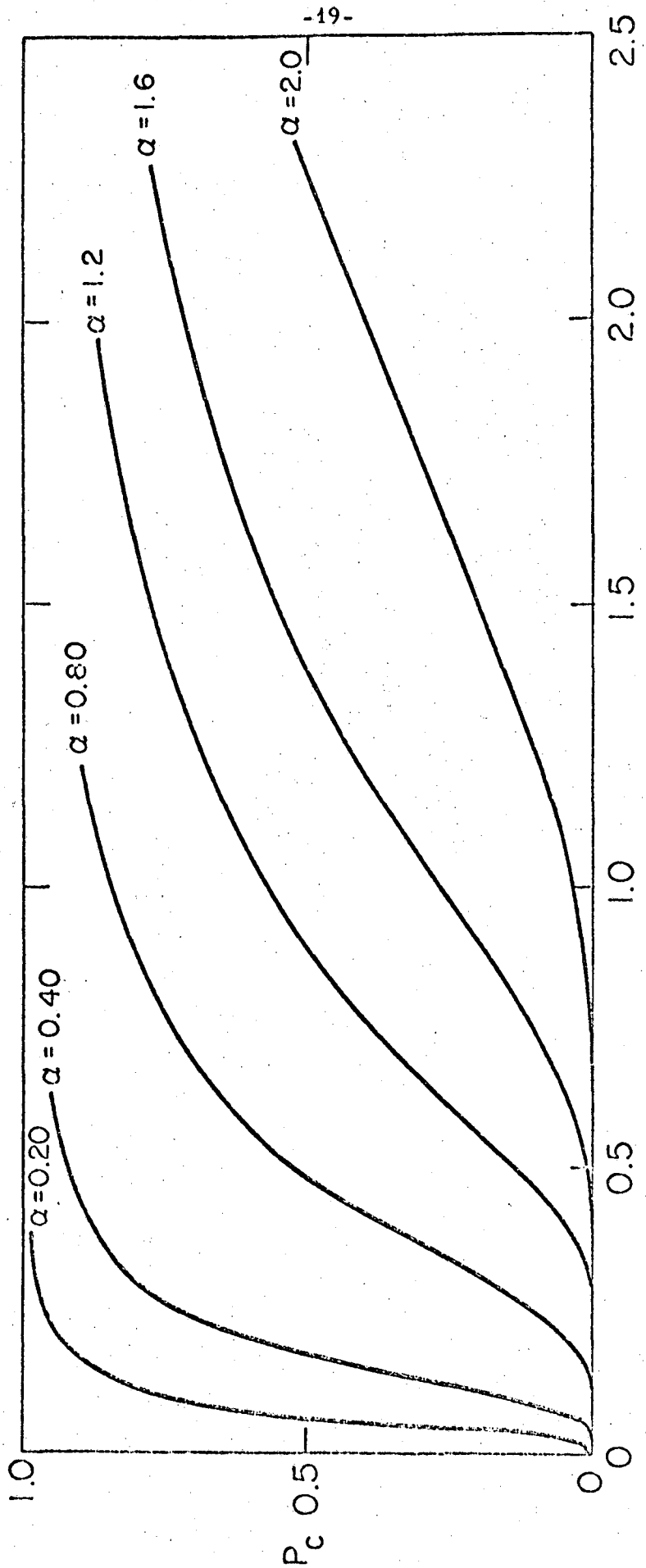
α=2.0
α=1.6
α=1.2
α=0.80
α=0.40
α=0.20
1.0
0.5
0
P_c
0
0.5
1.0
1.5
2.0
2.5
$\ell_s/R = \tau b \ell_s/\Gamma$

Fig. 3

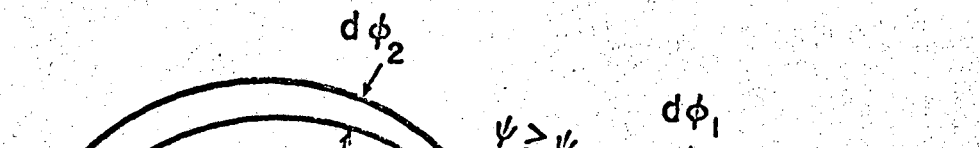

Fig. 4

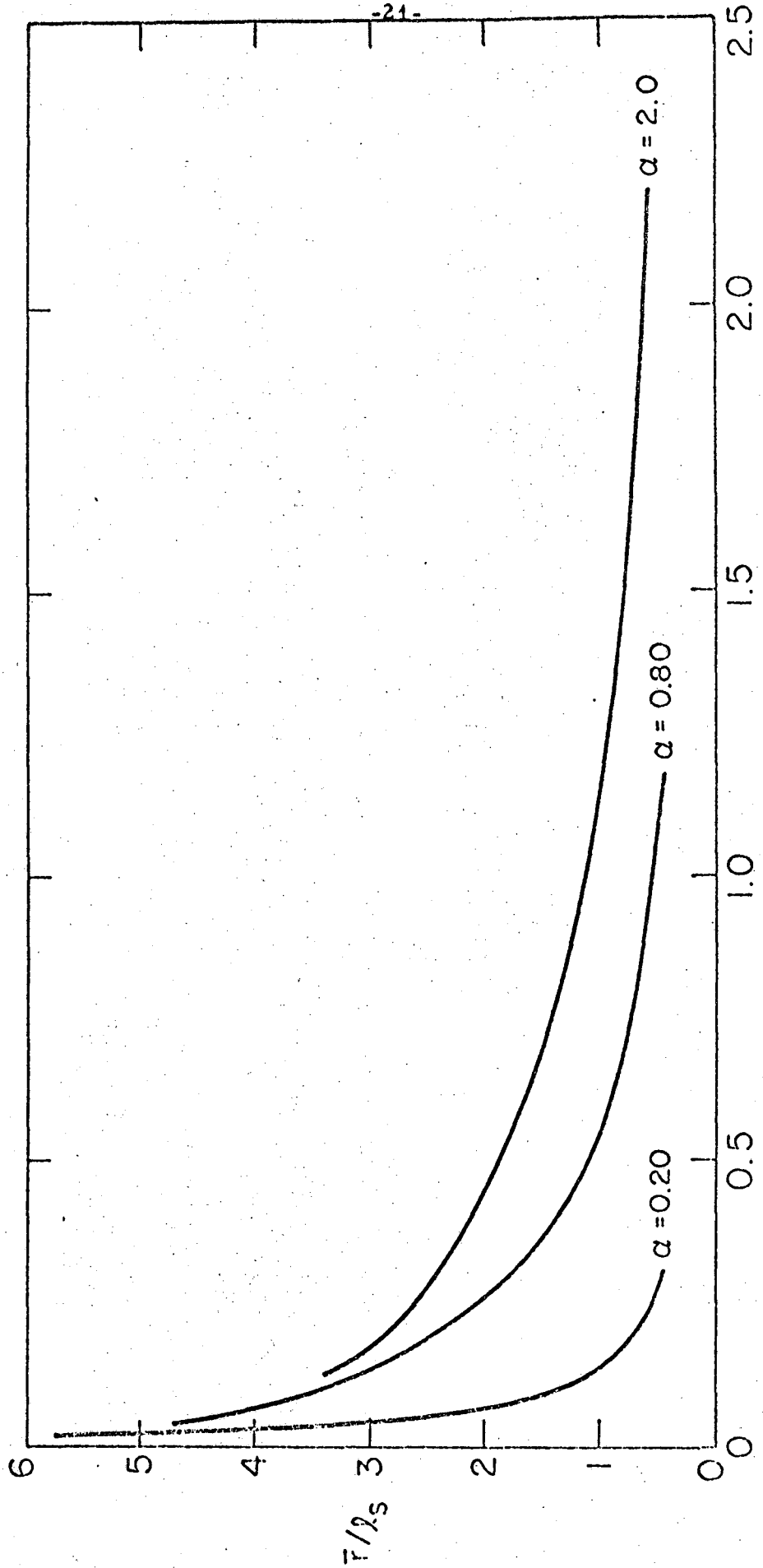
α = 2.0
α = 0.80
α =0.20
0
0.5
1.0
1.5
2.0
2.5
$\ell_s/R = \tau b \ell_s/\Gamma$
0
1
2
3
4
5
6
r/λ_s

Fig. 5

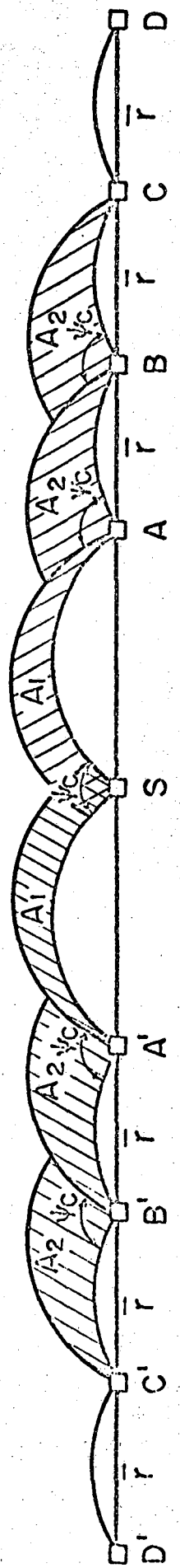

Fig. 6

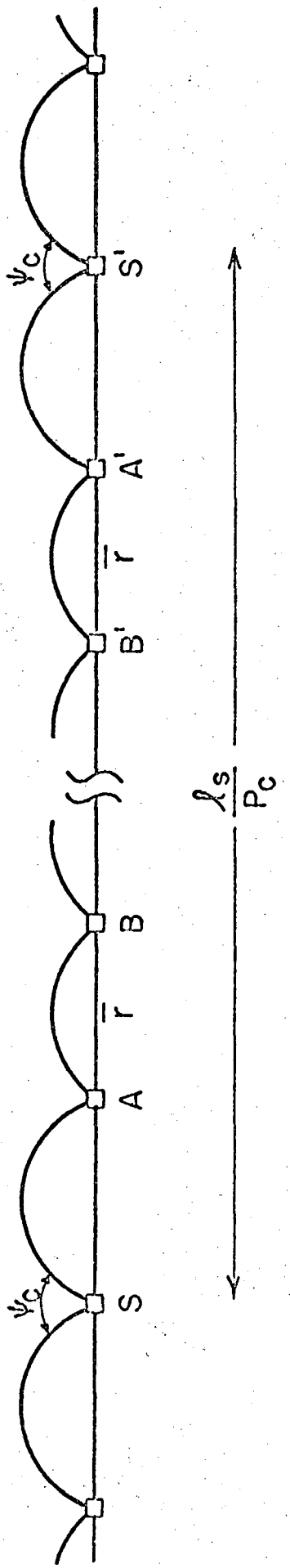

Fig. 7

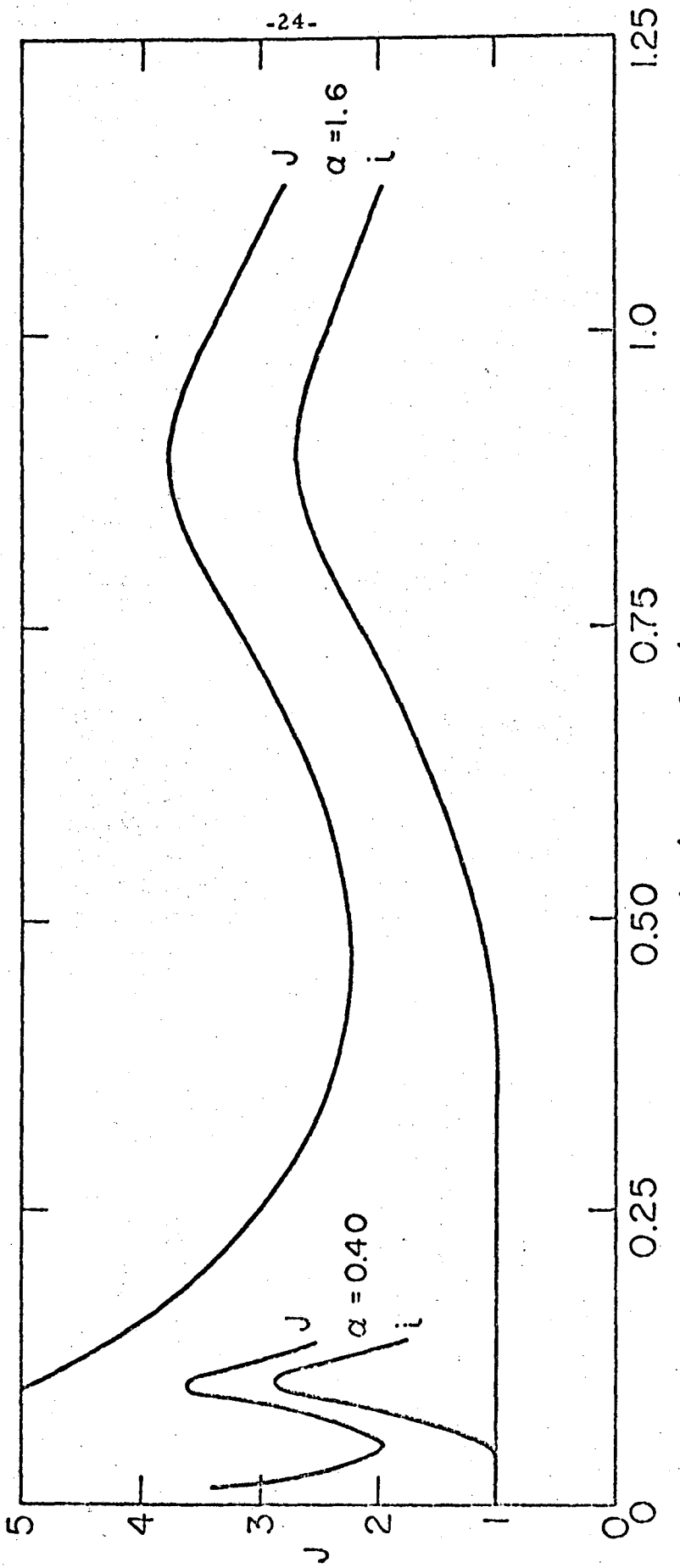
i, J
0
1
2
3
4
5
0
0.25
0.50
0.75
1.0
1.25
$\ell_s/R = \tau b \ell_s/\Gamma$
J
i
α = 1.6
J
i
α = 0.40

Fig. 8

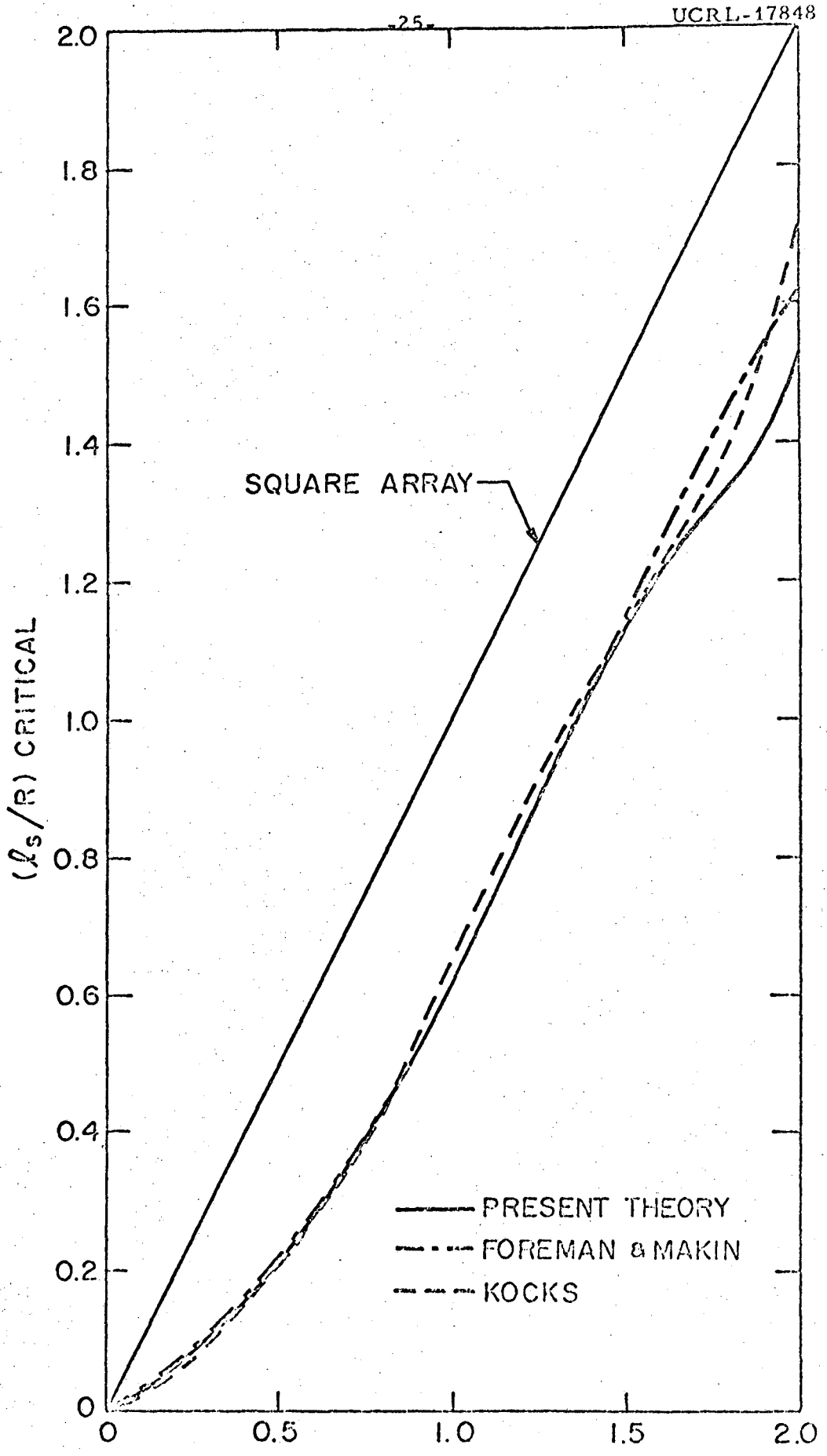
2.0
1.8
1.6
1.4
1.2
1.0
0.8
0.6
0.4
0.2
0
0
0.5
1.0
1.5
2.0
(ℓ_s/R) CRITICAL
α
SQUARE ARRAY
PRESENT THEORY
FOREMAN & MAKIN
KOCKS

Fig. 9

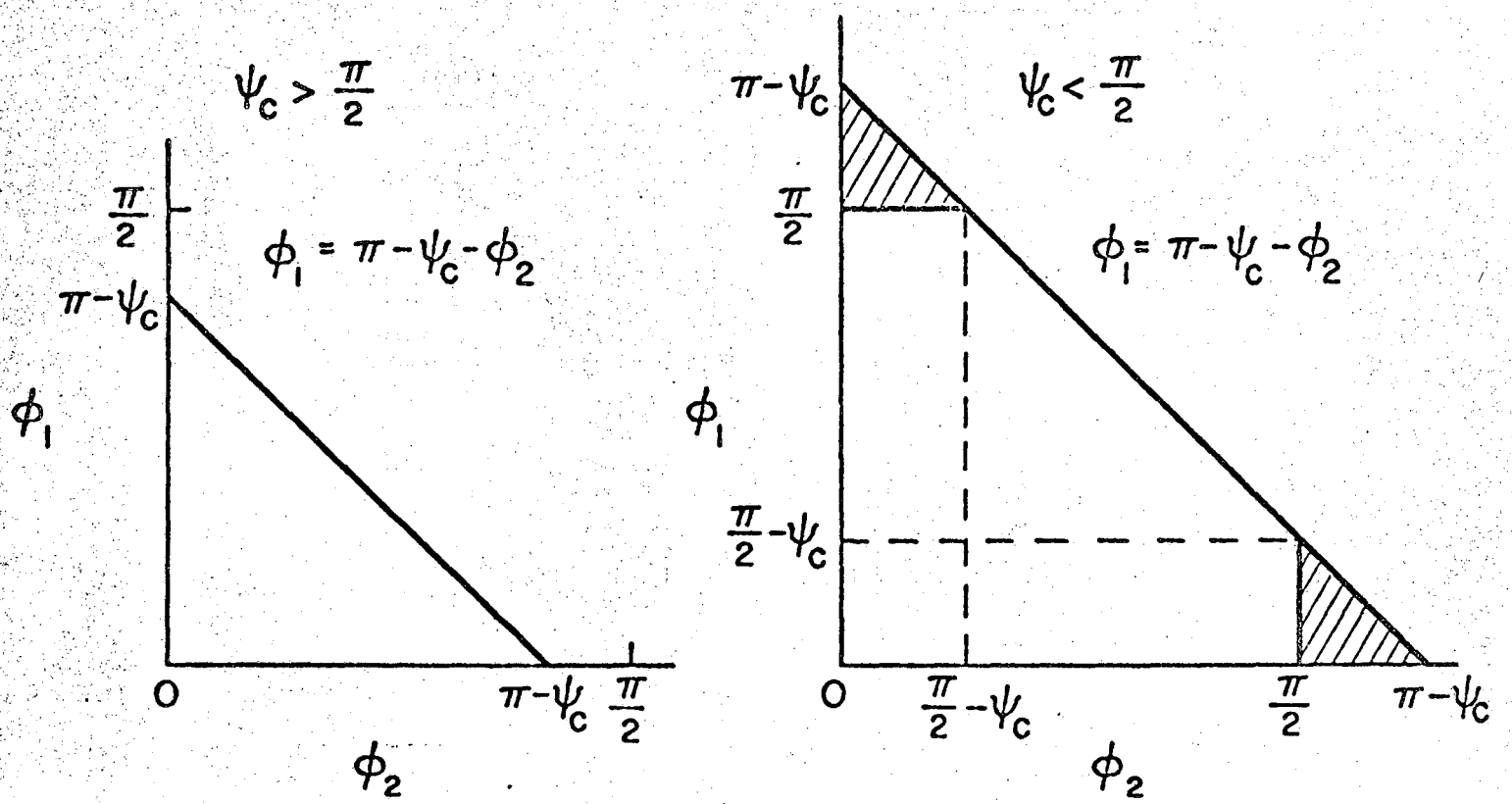
$\psi_c > \frac{\pi}{2}$
$\frac{\pi}{2}$
$\pi - \psi_c$
$\phi_1 = \pi - \psi_c - \phi_2$
ϕ_1
O
$\pi - \psi_c$
$\frac{\pi}{2}$
ϕ_2
$\pi - \psi_c$
$\psi_c < \frac{\pi}{2}$
$\frac{\pi}{2}$
$\phi_1 = \pi - \psi_c - \phi_2$
ϕ_1
$\frac{\pi}{2} - \psi_c$
O
$\frac{\pi}{2} - \psi_c$
$\frac{\pi}{2}$
$\pi - \psi_c$
ϕ_2

Fig. 10

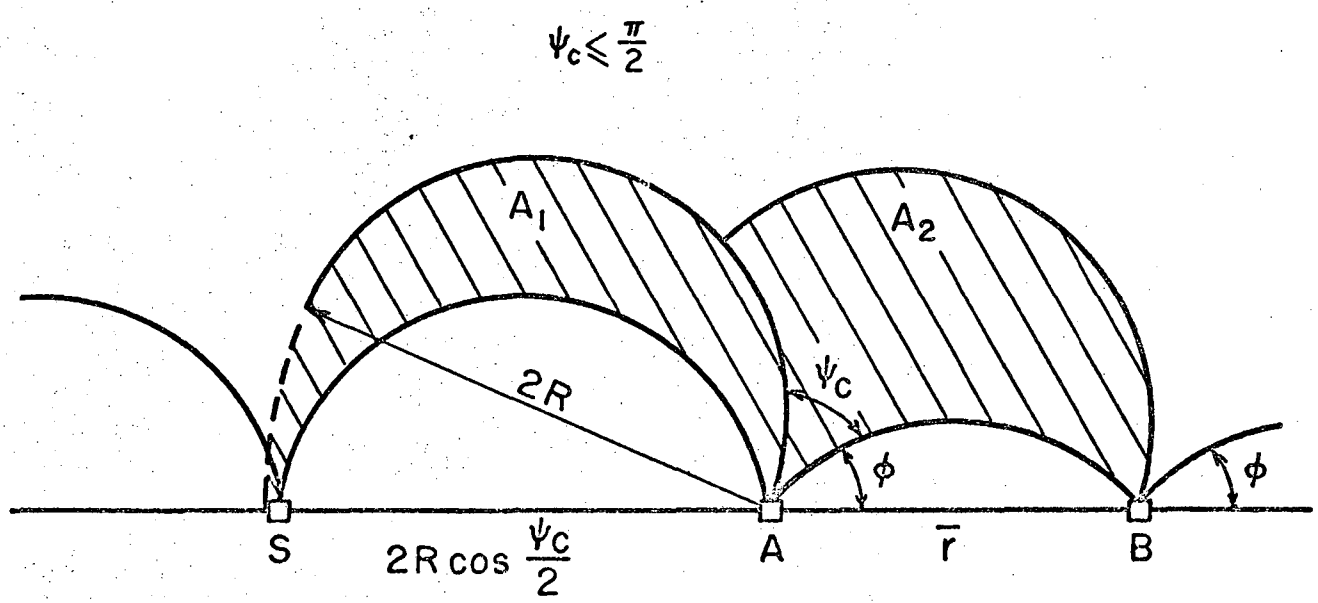
$\psi_c \leqslant \frac{\pi}{2}$
A_1
A_2
$2R$
ψ_c
ϕ
ϕ
S
$2R\cos\frac{\psi_c}{2}$
A
$\bar{r}$
B

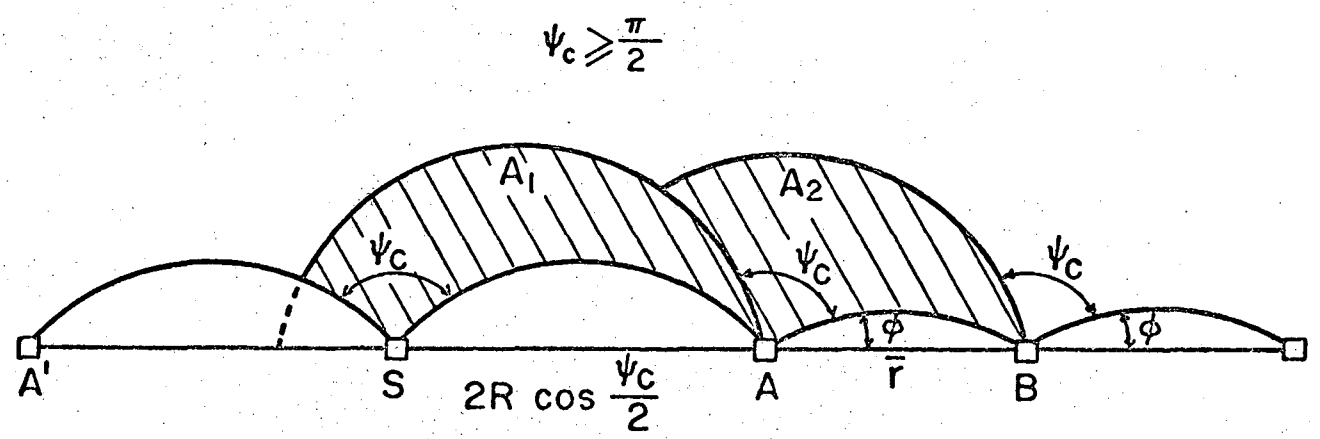
$\psi_c \geqslant \frac{\pi}{2}$
A_1
A_2
ψ_c
ψ_c
ψ_c
ϕ
ϕ
A'
S
$2R\cos\frac{\psi_c}{2}$
A
$\bar{r}$
B

Fig. 11